SF2A 2010
S. Boissier, M. Heydari-Malayeri, R. Samadi and D. Valls-Gabaud (eds)

EXOPLANET CHARACTERIZATION USING ANGULAR AND SPECTRAL DIFFERENTIAL IMAGING

A. Vigan[1], C. Moutou[1], M. Langlois[2], F. Allard[3], A. Boccaletti[4], M. Carbillet[5], D. Mouillet[6] and I. Smith[5]

Abstract. In the near future, new high-contrast imaging instruments dedicated to the direct detection of exoplanets at large orbital separations will be installed at the focus of large ground-based telescopes. Data obtained with these instruments optimized for very high contrast are strongly limited by the speckle noise. Specific observing strategies and data analysis methods, such as angular and spectral differential imaging, are required to attenuate the noise level and possibly detect the faint planet flux. Even though these methods are very efficient at suppressing the speckles, the photometry of the faint planets is dominated by the speckle residuals and it has a direct impact on the determination of the physical parameters of the detected planets. We present here the simulations that have been performed in the context of IRDIS, the dual-band imager of VLT-SPHERE, to estimate the influence of the photometric error on exoplanet characterization. In particular we show that the expected photometric performances will allow the detection and characterization of exoplanets down to the Jupiter mass at angular separations of 1.0" and 0.2" respectively around high mass and low mass stars with 2 observations in different filter pairs. We also show that the determination of the planets physical parameters from photometric measurements in different filter pairs is essentially limited by the error on the determination of the surface gravity.

Keywords: exoplanet, high-contrast imaging, instrument: VLT-SPHERE, IRDIS

1 Introduction

Most of the exoplanets currently known have been detected with indirect methods such as radial velocities or transits. Although these methods are mainly sensitive to planets at small orbital separations ($\lesssim 5$ AU), some stars are showing long-term trends that may indicate the presence of distant planetary companions. The wide use of adaptive optics systems on large ground-based telescopes has recently allowed to start probing for low mass companions at large orbital distances from nearby stars, leading to the image of the first exoplanet in 2005 around the young brown dwarf 2MASSW-J1207334-393254. In the following years, a handful of these objects have been imaged with existing instruments.

SPHERE (Spectro-Polarimetric High-conrast Exoplanet REsearch; Beuzit et al. 2006) is a second generation instrument for the VLT (Very Large Telescope) at ESO-Paranal Observatory which will be dedicated to the direct detection of exoplanets and low mass companions around nearby stars. Similar instruments are currently being built for other telescopes, such as GPI for Gemini South and HiCIAO for Subaru. This next generation of instruments aims at detecting young exoplanets down to the Jupiter mass (M_{Jup}) by reaching contrast values of 10^{-6} to 10^{-7} at angular separations as small as $\sim 0.1''$ with extreme adaptive optics systems and coronagraphy. SPHERE will have two scientific instruments working in the near-infrared: a diffraction-limited integral field spectrograph, and a differential spectro-imager (Dohlen et al. 2008), IRDIS. IRDIS will support several observing modes including Dual-Band Imaging (DBI) which will provide simultaneous images at two close wavelengths in

[1] LAM, UMR 6110, CNRS, Université de Provence, 38 rue Frédéric Joliot-Curie, 13388 Marseille Cedex 13, France
[2] CRAL, UMR 5574, CNRS, Université Lyon 1, 9 avenue Charles André, 69561 Saint Genis Laval Cedex, France
[3] CRAL, UMR 5574, CNRS, Université Lyon 1, ENS Lyon, 46 allée d'Italie, 69364 Lyon Cedex 07, France
[4] LESIA, UMR 8109, Obs. de Paris, CNRS, Université Paris-Diderot, 5 place Jules Janssen, 92195 Meudon Cedex, France
[5] Laboratoire Fizeau, UMR 6525, CNRS, Université de Nice, Obs. de la Côte d'Azur, Parc Valrose, 06108 Nice Cedex 2, France
[6] LAOG, UMR 5571, CNRS, Université Joseph-Fourier, BP 53, 38041 Grenoble Cedex 9, France

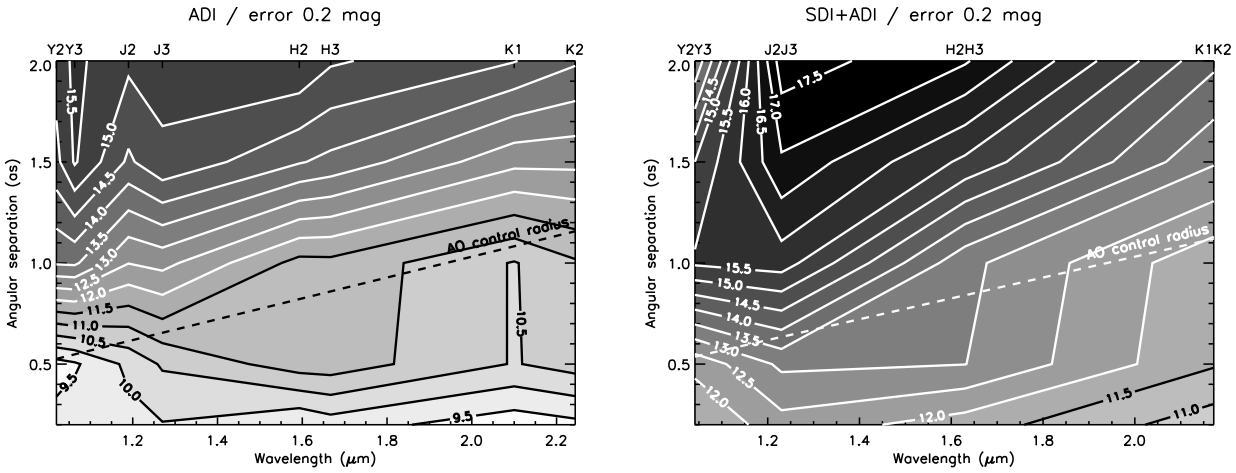

Fig. 1. Star-planet contrast at which a photometric precision of 0.2 mag is reached as a function of wavelength and angular separation for data analyzed with ADI (left) and SDI+ADI (right). Figures from Vigan et al. (2010).

one of its 5 different filter pairs covering Y to Ks bands. The IFS will be diffraction-limited in the near-infrared and will provide spectra from Y to H bands.

An end-to-end model of the SPHERE instrument has been developed to test the performances of the instrument (Carbillet et al. 2008). This code, written in IDL, includes a large number of effects at different spatial and temporal scales. It allowed us to simulate a realistic 4 hours observation sequence with IRDIS of a star at a declination $\delta = -45°$ covering hour angles of -2 hr to +2 hr with an anodized pupil Lyot coronagraph. Fake planets have been introduced into the data cubes, and photometry was calculated to represent different planetary systems with contrast values from ∼15 to ∼17.5 mag. These data cubes have been used to study the photometric accuracy, which can be expected after using different data analysis methods, and the consequences in terms of mass estimation of the detected objects.

2 Photometric accuracy

Data analysis methods are necessary to attenuate the quasi-static speckle noise, which is an intrinsic limit in high-contrast images (Soummer et al. 2007). We used three different methods: Spectral Differential Imaging (SDI; Racine et al. 1999), Angular Differential Imaging (ADI; Marois et al. 2006) and their combination (SDI+ADI). The flux of the detected objects in the different data cubes analyzed with these methods has been estimated with aperture photometry an compared to the original value to measure the photometric error.

Figure 1 presents the photometric performance which can be expected for 5-σ detections: It shows the star-planet contrast at which a 0.2 mag precision is reached as a function of wavelength and angular separation, for ADI and SDI+ADI data analysis methods. Two interesting effects are visible: (1) the photometric performance clearly depends on wavelength, and (ii) there are two different regimes depending on the position compared to the AO control radius. The first effect is directly related to the chromaticity of the PSF: in speckle-limited regime the noise attenuation is almost constant with angular separation compared to the corona graphic profile, and the level of the coronagraphic profile linearly depends on wavelength. The second effect is related to the AO correction inside the control radius. Inside that region we see a stabilization of the performance, while outside, the photometric performance increases almost linearly with angular separation at all wavelengths. These effects are more visible with ADI because in the case of SDI+ADI, a large part of the chromatic effects have been removed by the SDI part of the analysis.

3 Characterization performances

These empirical photometric performances have then been used to estimate the characterization capabilities of IRDIS in DBI mode. We have created a new simulation in which we have tested for a large number of planetary atmosphere models our ability to determine the physical parameters T_{eff} (effective temperature) and log g (surface gravity) of the objects. The principle of this simulation was to create a planetary system defined

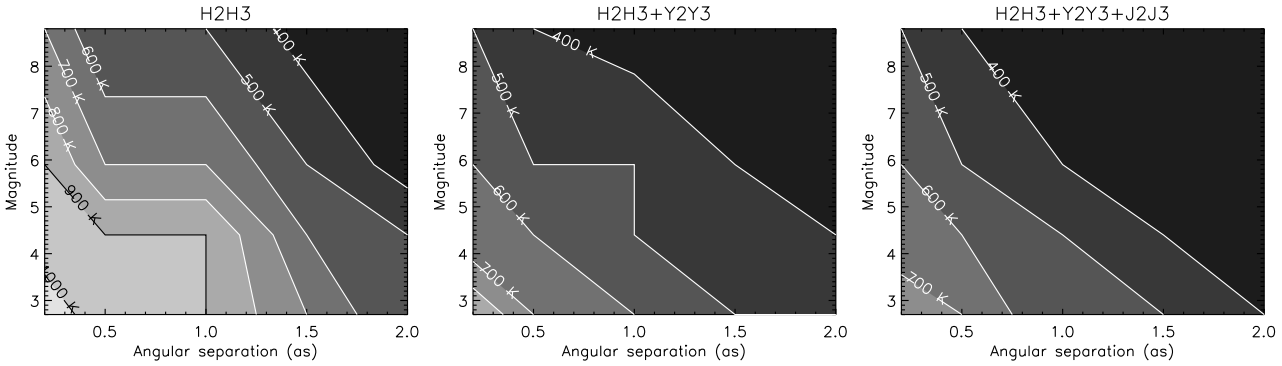

Fig. 2. Lowest T_{eff} which can be estimated as a function of angular separation and star V magnitude for observations with different filter pairs: H2H2 (left), H2H3+Y2Y3 (center) and H2H3+Y2Y3+J2J3 (right). Figure based on Vigan et al. (2010).

by the star magnitude (spectral type) and the planet T_{eff}/log g, simulate an observation with different filter pairs, introduce a photometric error, and try to find out which planet model was used at the beginning of the simulation. All the possible filter pair combinations of IRDIS have been tested with a large sample of planetary atmosphere models (Allard et al. 2001, 2003, 2010 in preparation; Burrows et al. 2006).

This simulation allowed us to set priorities on the different filter pairs of IRDIS for faint objects characterization. H2H3 has the highest priority, followed by Y2Y3/J2J3 and H3H4/K1K2. These priorities are defined for characterization with no *a priori* information. For example, K1K2 or H3H4 filter pairs may reveal to be more interesting when the object is known to be warm. We have studied the lowest planet T_{eff}, which can be estimated using observations with different filter pairs. The results are showed in Fig. 2 where the lowest T_{eff} estimable is given as a function of angular separation and star V magnitude for filter pairs H2H3, H2H3+Y2Y3 and H2H3+Y2Y3+J2J3. We clearly see that using two or three filter pairs brings a large improvement. When using only H2H3, planets with T_{eff} down to 900 K should be characterized at an angular separation of 0.2″ from bright stars and 700 K from fainter stars. Adding a second filter pair considerably improves these results by 200 K, while adding a third pair confirms these limiting values.

With the considered data analysis methods and according to the evolutionary models from Baraffe et al. (2003) for the COND atmosphere models, we can estimate that in a very young system of 10 Myr, we should be able to characterize a planet of 1 M_{Jup} with H2H3 at separations larger than 0.5″ around a low mass star (M0 at 10 pc) where the star-planet contrast is favorable, but only further than 2.0″ around a bright star (F0 at 10 pc) where the contrast difference is larger. With two filter pairs, the limit would be 0.2″ around a faint star and 1.0″ around bright star. For older systems, only planets of a few masses of Jupiter could be characterized. At 100 Myr, a Jupiter mass planet would remain out of reach for characterization with H2H3 filters around a bright star, and only at separations larger than 1.5″ around fainter stars.

Finally, we have studied the impact of errors on the determination of T_{eff} and log g for hypothetical 2 M_{Jup} planets orbiting at 5 A.U. from M0 and F0 stars at 10 pc aged of 44 ± 30 Myr (average age and errors for young stars in the preliminary SPHERE target sample). According to the evolutionary models from Baraffe et al. (2003), such planets should have $T_{eff} = 516$ K and log $g = 3.54$ dex, resulting in a contrast of 11.9 mag and 15.6 mag in H band respectively around the M0 and F0 stars. Around a faint star, the parameters T_{eff} and log g are estimated with an accuracy close to the one given by the atmosphere model grid ($1.9^{+1.3}_{-0.7}$ M_{Jup}), leading to an estimation of $1.9^{+1.2}_{-1.0}$ M_{Jup}. Around a high mass star, the planet is very close to the detection limit at 0.5″, resulting in a poor estimation of both T_{eff} and log g: the important photometric error in H2H3 leads to a very large uncertainty on log g (4.33 ± 1.23). The mass of the planet is then estimated to $1.1^{+2.6}_{-0.5}$ M_{Jup}.

4 Conclusion

We have studied the performances of IRDIS, the dual-band imager and spectrograph of SPHERE, for the characterization of faint planetary companions. We have performed detailed end-to-end numerical simulation to obtain realistic data cube representing various planetary systems, which we have used to study the photometric accuracy when using ADI and SDI+ADI data analysis methods. Using the best possible filter pairs sequence, we

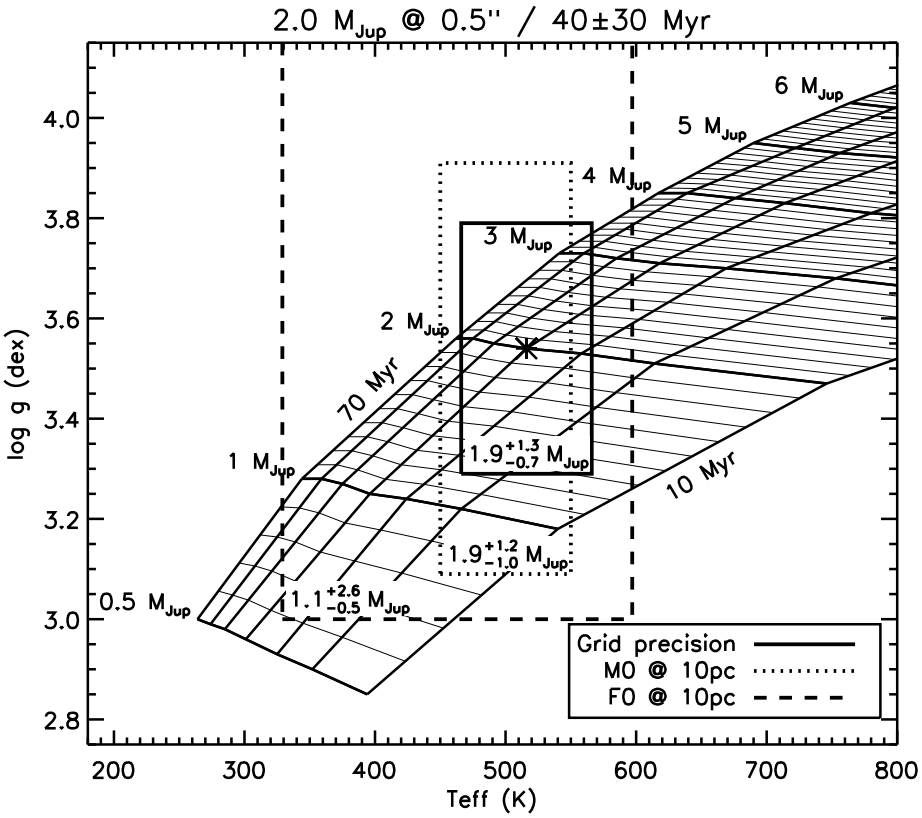

Fig. 3. Isochrones for the COND planetary atmosphere models covering an age of 40 ± 30 Myr used for the determination of the mass of hypothetical 2 M_{Jup} planets orbiting at 5 A.U. from M0 and F0 stars at 10 pc. The error boxes defined by the possible values for T_{eff} and log g of both planets are respectively represented by dotted and dashed rectangles. The position of the planet predicted by the evolutionary models is represented by the star symbol, and the error box defined by the atmosphere models grid precision is given by a plain rectangle. Figure from Vigan et al. (2010).

have studied the lowest T_{eff} of planet which can be estimated, concluding that we should be able to characterize a planet of 1 M_{Jup} with H2H3+Y2Y3 pairs at separations larger than $0.2''$ around a low mass star (M0 at 10 pc) where the star-planet contrast is favorable, but only further than $1.0''$ around a bright star (F0 at 10 pc). Finally, we have studied the impact of errors on T_{eff} and log g on the estimation of the planet mass. Around faint low mass stars, we should be able to almost reach the precision of the model grids, while around bright stars the large photometric error is a significant limitation to the accurate determination of the planet mass.

References

Allard, F., Guillot, T., Ludwig, H.-G., et al. 2003, in IAU Symposium, Vol. 211, Brown Dwarfs, ed. E. Martín, p. 325

Allard, F., Hauschildt, P. H., Alexander, D. R., Tamanai, A., & Schweitzer, A. 2001, ApJ, 556, 357

Baraffe, I., Chabrier, G., Barman, T. S., Allard, F., & Hauschildt, P. H. 2003, A&A, 402, 701

Beuzit, J.-L., Feldt, M., & Dohlen, K. e. a. 2006, The Messenger, 125, 29

Burrows, A., Sudarsky, D., & Hubeny, I. 2006, ApJ, 640, 1063

Carbillet, M., Boccaletti, A., & Thalmann, C. e. a. 2008, in SPIE Conference Series, Vol. 7015

Dohlen, K., Langlois, M., & Saisse, M. e. a. 2008, in SPIE Conference Series, Vol. 7014

Marois, C., Lafrenière, D., Doyon, R., Macintosh, B., & Nadeau, D. 2006, ApJ, 641, 556

Racine, R., Walker, G. A. H., Nadeau, D., Doyon, R., & Marois, C. 1999, PASP, 111, 587

Soummer, R., Ferrari, A., Aime, C., & Jolissaint, L. 2007, ApJ, 669, 642

Vigan, A., Moutou, C., Langlois, M., et al. 2010, MNRAS, 407, 71